Dolphin, D., Muljiani, Z., Rousseau, K., Borg, D. C., Fajer, J., & Felton, R. H. (1973) *Ann. N.Y. Acad. Sci. 206*, 177–200.
Dunford, H. B., & Stillman, J. S. (1976) *Coord. Chem. Rev. 19*, 187–251.
Fajer, J., Borg, D. C., Forman, A., Felton, R. H., Vegh, L., & Dolphin, D. (1973) *Ann. N.Y. Acad. Sci. 206*, 349–364.
Foote, N., Gadsby, P. M. A., Berry, M. J., Greenwood, C., & Thomson, A. J. (1987) *Biochem. J. 246*, 659–668.
Gasyna, Z., Browett, W. R., & Stillman, M. J. (1984) *Inorg. Chem. 23*, 382–386.
Groves, J. T., Haushalter, R. C., Nakamura, M., Nemo, T. E., & Evans, B. J. (1981) *J. Am. Chem. Soc. 103*, 2884–2886.
Law, A. Y. C. (1978) B.Sc. (Honors) Research Thesis, University of Western Ontario.
Magonov, S. N., Arutjunjan, A. M., Blumenfeld, L. A., Davydov, R. M., & Sharonov, Yu. A. (1977) *Dokl. Akad. Nauk. SSSR 232*, 695–698.
Magonov, S. N., Blumenfeld, L. A., Davydov, R. M., Arutjunjan, A. M., & Sharonov, Yu. A. (1978) *Mol. Biol. (Moscow) 12*, 1191–1197.
McIntosh, A. R., & Stillman, M. J. (1977) *Biochem. J. 167*, 31–37.
Nadezhdin, A. D., & Dunford, H. B. (1979) *Photochem. Photobiol. 29*, 889–903.
Nyokong, T., Gasyna, Z., & Stillman, M. J. (1987) *Inorg. Chem. 26*, 1087–1095.
Oertling, W. A., & Babcock, G. T. (1985) *J. Am. Chem. Soc. 107*, 6406–6407.
Schatz, P. N., Mowery, R. L., & Krausz, E. R. (1978) *Mol. Phys. 35*, 1537–1557.
Schulz, C. E., Devaney, P. W., Winkler, H., Debrunner, P. G., Doan, N., Chiang, R., Rutter, R., & Hager, L. P. (1979) *FEBS Lett. 103*, 102–105.
Schulz, C. E., Rutter, R., Sage, J. T., Debrunner, P. G., & Hager, L. P. (1984) *Biochemistry 23*, 4743–4754.
Sharonov, Yu. A., Minayev, A. P., Livshitz, M. A., Sharonova, N. A., Zhurkin, V. B., & Lysov, Yu. P. (1978) *Biophys. Struct. Mech. 4*, 139–158.
Springall, J., Stillman, M. J., & Thomson, A. J. (1976) *Biochim. Biophys. Acta 453*, 494–501.
Stillman, J. S., Stillman, M. J., & Dunford, H. B. (1975a) *Biochem. Biophys. Res. Commun. 63*, 32–35.
Stillman, J. S., Stillman, M. J., & Dunford, H. B. (1975b) *Biochemistry 14*, 3183–3188.
Teraoka, J., Ogura, T., & Kitagawa, T. (1982) *J. Am. Chem. Soc. 104*, 7354–7356.
Thomson, A. J., & Johnson, M. K. (1980) *Biochem. J. 191*, 411–420.
Thomson, A. J., Johnson, M. K., Greenwood, C., & Gooding, P. E. (1981) *Biochem. J. 193*, 687–697.
Van Wart, H. E., & Zimmer, J. (1985) *J. Am. Chem. Soc. 107*, 3379–3381.
Vickery, L., Nozawa, T., & Sauer, K. (1976) *J. Am. Chem. Soc. 98*, 343–350.

Femtosecond Charge Separation in Organized Assemblies: Free-Radical Reactions with Pyridine Nucleotides in Micelles

Y. Gauduel,* S. Berrod, A. Migus, N. Yamada, and A. Antonetti
Laboratoire d'Optique Appliquée, INSERM U275, Ecole Polytechnique-ENSTA, 91120 Palaiseau, France
Received July 15, 1987; Revised Manuscript Received November 24, 1987

ABSTRACT: Femtosecond laser UV pulse-induced charge separation and electron transfer across a polar interface have been investigated in anionic aqueous micelles (sodium lauryl sulfate) containing an aromatic hydrocarbon (phenothiazine). The early events of the photoejection of the electron from the micellized chromophore and subsequent reaction of electron with the aqueous perimicellar phase have been studied by ultrafast infrared and visible absorption spectroscopy. The charge separation (chromophore^{+}···e^{-}) inside the micelle occurs in less than 10^{-13} s (100 fs). The subsequent thermalization and localization of the photoelectron in the aqueous phase are reached in 250 fs. This results in the appearance of an infrared band assigned to a nonrelaxed solvated electron (presolvated state). This transient species relaxes toward the fully solvated state of the electron in 270 fs. In anionic aqueous micelles containing pyridine dinucleotides at high concentration (0.025–0.103 M), a single electron transfer can be initiated by femtosecond photoionization of phenothiazine. The one-electron reduction of the oxidized pyridine dinucleotide leads to the formation of a free pyridinyl radical. The bimolecular rate constant of this electron transfer depends on both the pH of the micellar system and the concentration of oxidized acceptor. The free-radical reaction is analyzed in terms of the time dependence of a diffusion-controlled process. In the first 2 ps following the femtosecond photoionization of PTH inside the micelle, an early formation of a free pyridinyl radical is observed. This suggests that an ultrafast free-radical reaction with an oxidized form of pyridine nucleotide can be triggered by a single electron transfer in less than 5×10^{11} s^{-1}.

Intensive studies have produced a substantial body of information concerning reactions between solvated electron and chemical or biological acceptors in homogeneous aqueous solutions (Anbar & Neta, 1967, 1968; Land & Swallow, 1968; Anbar, 1969; Lichtin et al., 1973; Dainton, 1975; Klapper & Faraggi, 1983). The knowledge of absolute rate constant is of prime importance for a proper understanding of the chemical reactions. In particular, the studies of one-electron-transfer reactions in concentrated solutions of biomolecules (coenzymes, amino acids) should permit apprehension of the mechanisms

* Author to whom correspondence should be addressed.

0006-2960/88/0427-2509$01.50/0

of free-radical reactions occurring in components of living cells.

The investigations, by a picosecond pulse radiolysis system, of fast reactions involving hydrated electrons in concentrated solutions have allowed clarification of the influence of time dependence, Coulombic interactions, or ionic strength on the bimolecular rate constant of diffusion-controlled reactions (Bronskill et al., 1970; Wolff et al., 1970; Aldrich et al., 1971; Schwartz, 1971; Czapski & Peled, 1973; Lam & Hunt, 1975). However, the radiation chemistry performed up to now did not permit elucidation of the early fast events of free-radical reactions occurring in less than 20–30 ps (Chase & Hunt, 1975; Jonah et al., 1975, 1977; Duplatre & Jonah, 1985; Lewis & Jonah, 1986).

The laser photolysis has been undertaken to investigate charge transfer (electron or proton) in homogeneous and heterogeneous solutions (Richards et al., 1970; Grätzel & Thomas, 1974; Moroi et al., 1979; Thomas, 1980; Pileni, 1981; Visser & Fendler, 1982).

Recent technological advances in ultrashort laser pulses (Fork et al., 1982; Migus et al., 1982) now allow such studies with femtosecond accuracy. In concentrated solutions, there is now indirect evidence that e^-_{sol}[1] is not the unique reductant species which can trigger a one-electron transfer. It has been suggested that precursors of solvated electron would initiate free-radical reactions in concentrated media (Aldrich et al., 1971; Lam & Hunt, 1975; Wolff et al., 1970; Jonah et al., 1977; Lewis & Jonah, 1986). Indirect methods including the study of initial yields of solvated electron or the determination of the "C_{37}" values of a scavenger have been developed to investigate the free-radical reactions triggered by precursors of e^-_{sol} (Razem & Hill, 1977). Up to now a direct characterization of a precursor of e^-_{sol} was not possible by classical spectroscopic techniques, and little is known about the precursors of e^-_{sol} in polar solutions. A more decisive investigation of reactions involving presolvated electrons in aqueous environment compels the direct observation and characterization of precursors of e^-_{sol}.

Following these ideas the goal of this work was to investigate the early steps of photochemical generation of hydrated electrons in organized assemblies and the monoelectronic transfer on biological acceptors (oxidized pyridine nucleotides). Much of the interest in oxidized NAD^+ derives from its function in the two-electron reaction mechanism in biological oxidation–reduction chains ($NAD^+ + 2e^- + H^+ \rightleftarrows NADH$). A mechanism of sequential monoelectronic transfer cannot be excluded (Land & Swallow, 1968; Bielski et al., 1983). These redox reactions may trigger the formation of a free pyridinyl radical of great biochemical importance ($NAD^•$). In concentrated solutions, the pathway of reduction reactions of the key coenzyme (NAD^+) remains to be clarified.

Aqueous micelles are particularly good candidates for such investigations owing to the fact that they permit the reorganization of reactants (electron donor or acceptor) at a molecular level. The photoejection of an electron from micellized PTH to the aqueous phase is initiated by femtosecond UV pulses. The early steps of intramicellar charge separation can be described by

$$PTH_M \xrightarrow{h\nu} PTH^*_M \rightarrow [PTH^+\cdots e^-]_M \rightarrow PTH^+_M + e^-_{qf} \quad (1)$$

$$e^-_{qf} + n(H_2O) \rightarrow e^-\cdots n(H_2O) \rightarrow e^-_{presol}\ (IR) \quad (2)$$

$$e^-_{presol} \rightarrow n(H_2O)^- \simeq e^-_{sol} \quad (3)$$

Free-radical reactions coupled to the reactivity of e^-_{sol} have been investigated in the organized redox complex PTH/micelle/water–pyridine nucleotide. The range of oxidized coenzyme concentration (0.025–0.1 M) used in this work permits (i) study of the one-electron-transfer reaction in relation to that with the protonated form of pyridinium ions (pH effect) and (ii) analysis of free-radical reactions at intermediate concentrations range where the rate constant is changing from dilute to concentrated solution.

Experimental Procedures

Preparation of Biomicellar Samples. Anionic aqueous micelles are prepared by dispersing phenothiazine (2×10^{-4} M) in sodium lauryl sulfate solution ([NaLS] = 0.07 M). The blend is gently stirred at 55–60 °C during 4 h to obtain complete integration of the probe and a clear solution. During this stage, care is taken to exclude light. Taking into account the cmc (7×10^{-3} M) and the mean aggregation number (65) (Zana et al., 1981), the calculated micellar concentration is 9.5×10^{-4} M. NaLS (from Serva) was purified by adding 50 g to 100 mL of warm methanol. The mixture was then cooled, filtered, and dried in vacuum. Bideionized water was doubly distilled in a quartz distillator with $KMnO_4$. At 296 K, the resistivity is greater than 19 MΩ. PTH (from Merck) was of puriss quality and used as received. The concentration of the micellized chromophore was determined by spectrophotometric measurements, assuming that the variation of the solute extinction coefficient on going from a homogeneous to a micellar solution could be neglected. Anionic biomicellar systems containing oxidized nucleotides have been cautiously prepared by integrating NAD^+ or NMN^+ in the aqueous phase of NaLS (0.07 M) micelles ([PTH] = 2×10^{-4} M). The concentration of the oxidized nucleotides in biomicelles was in the range 0.025–0.11 M. NAD^+ and NMN^+, from Sigma Chemical Co., St. Louis, MO, were of the highest purity available (purity higher than 99.8% by high-pressure liquid chromatography). Micellar assemblies at pH 6.8 were buffered with Tris–EDTA–borate buffer (from Sigma) at a final concentration of 0.020 M. Acid micelles containing nucleotides (pH 2.7) were obtained without buffer.

Before experiments, all the micellar samples were maintained at 22 ± 1 °C and deoxygenated by tonometry, with high-purity nitrogen gas. Static spectral characterization of micellar samples was run on a dual-beam Varian 2300 spectrophotometer in the UV and visible spectral regions.

Photoionization Procedure and Time-Resolved Absorption Spectroscopy. Time-resolved absorption spectroscopy schemes have been described in detail elsewhere (Migus et al., 1985). A passively mode locked dye ring laser, generates a pulse of typically 50-fs duration at a wavelength of 620 nm. Amplification of these pulses is achieved with a four-stage dye amplifier pumped by a Q-switched frequency-doubled neodynium Yag laser. This setup finally produces 1-mJ pulses of 100-fs duration at 620 nm with a repetition rate of 10 Hz.

This initial 620-nm beam was split in two parts: one was the pump beam which passes through a variable-delay line driven by a stepping motor and was focused into a 1.5-mm KDP crystal to produce up to a 20-μJ, 100-fs pulse at 310 nm. This beam was used to initiate photochemical process, i.e., the photoionization of the chromophore embedded in the micellar system (reactions 1–3). The other 620-nm beam was focused into a water cell, converted to a white light continuum, and split in two parts: one probed the excited region of the sample,

[1] Abbreviations: cmc, critical micellar concentration; NaLS, sodium lauryl sulfate; PTH, phenothiazine; NAD^+, nicotinamide adenine dinucleotide (oxidized); NMN^+, nicotinamide mononucleotide; AMP, adenosine 5′-monophosphate; e^-_{qf}, quasi free electron; e^-_{presol}, infrared presolvated electron; pre-e^-_{sol}, precursor of solvated electron; e^-_{sol}, solvated electron; $Pyr^•$, pyridinyl radical; Pyr^+, pyridinium ion; EDTA, ethylenediaminetetraacetic acid; Tris, tris(hydroxymethyl)aminomethane.

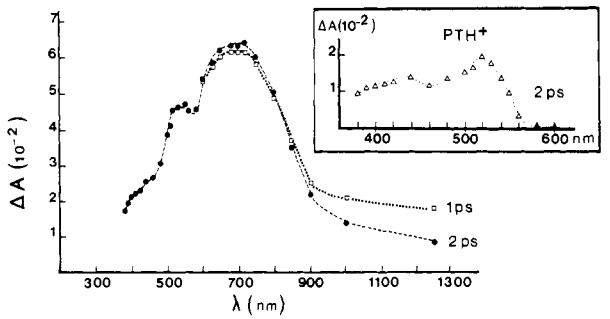

FIGURE 1: Transient absorption spectra from femtosecond laser photoionization of deoxygenated anionic aqueous micelles ([PTH] = 2×10^{-4} M; [NaLS] = 0.07 M, pH 6.5). The points are calculated from the experimental kinetics at different wavelengths. The insert shows the differential spectra of PTH^+, 2 ps after the femtosecond photoionization of PTH.

while the other missed the sample and is used as a reference. The signals corresponding to the probe and reference pulse energies at a given wavelength were sent through an electronic chain to a computer. Typically over 50 000 pulses are taken into account in kinetic curves. Their ratio was determined and used in a multichannel analyzer program. The transient species following the photoionization step were then directly observed by monitoring the sample optical densities as a function of wavelength and time delay.

The photochemical reactions took place in a fixed-volume cell (2-mm path length) translated in a vertical plane and perpendicular to the propagation of the light beams, so that each pulse at a 10-Hz repetition rate excited a new region of the sample. To avoid accumulation of final products, biomicellar systems were changed every 2 h.

RESULTS

Initial Charge Separation and Formation of Hydrated Electron. The absorption changes obtained from the femtosecond photoionization of micellized phenothiazine (2×10^{-4} M) are shown in Figure 1. One picosecond after the femtosecond UV pulse, the transient spectrum between 380 and 1250 nm is not yet stabilized: a tail of an infrared band extending above 1250 nm can be still observed, and in the visible spectral region the broad band peaking around 720 nm (1.7 eV) is not fully developed. Two picoseconds after excitation, the IR band has totally disappeared. Concurrently, the structureless and unsymmetric band extending a high-energy tail above 3 eV is similar to the known e^-_{sol} one. The infrared wing is assigned to a localized or presolvated state of electron in the aqueous phase of anionic micelles. The transitory spectrum observed 1 ps after the pulse excitation shows a hump peaking around 520 nm. A differential spectrum also shows the existence of an other hump around 430 nm (Figure 1B). From the available data literature, we assigned these two bands to the cationic radical PTH^+.

A careful analysis of the kinetic data obtained in the infrared and visible spectral region has been performed with a model which takes into account the existence of two populations: one absorbing in the infrared appears with a time constant T_1 and then relaxes toward the solvated state with a time constant T_2. At 1250 and 720 nm, the kinetics could be well fitted with the same T_1 and T_2 values by numerically convoluting these responses with the pump and probe temporal profile. One key point in these experiments is the determination for each probe wavelength of both the instrumental instantaneous response and the so-called zero time delay. A detailed description of this procedure has been published elsewhere (Gauduel et al., 1985).

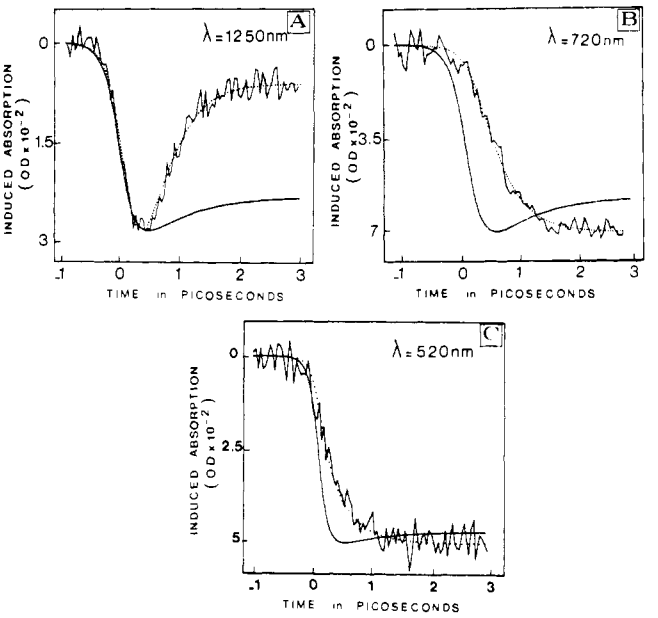

FIGURE 2: Rise time of induced absorption at 1250, 720, and 520 nm following photoionization of PTH (2×10^{-4} M) in micellar systems (0.07 M NaLS) with a 100-fs laser pulse (λ = 310 nm, $h\nu$ = 4 eV). The instantaneous responses (—) are defined by recording an induced absorption after excitation of liquid *n*-heptane. The smooth lines represent the computed best fit of experimental traces. (A) Localized prehydrated electron with an appearance time (T_1 = 250 ± 20 fs) and a lifetime (T_2 = 270 ± 20 fs) as observed in the near-infrared. (B) Hydrated electron appearance assuming the same time constants. (C) Induced absorption at 520 nm including the combination of the instantaneous appearance of PTH^+ and the rise of e^-_{sol} as measured at 720 nm.

The curve of the Figure 2A shows that the kinetics in the infrared region is well fitted with the equation $A_{(t)} = A^0[1/(T_2 - T_1)][\exp(-t/T_2) - \exp(-t/T_1)]$ giving an appearance time of 250 ± 20 fs and a lifetime T_2 = 270 ± 20 fs. The incomplete recovery of the signal at 1250 nm is due to a weak contribution of the e^-_{sol} absorption. At 720 nm (Figure 2B), the induced absorption is perfectly fitted to the convolution of the pulse profile and the expected signal rise $A_{(t)} = A^0[1 - 1/(T_2 - T_1)][T_2 \exp(-t/T_2) - T_1 \exp(-t/T_1)]$, by use of the same values of T_1 and T_2 as determined at 1250 nm. At 520 nm (Figure 2C), the curves can be well fitted to a combination of an instantaneous component due to PTH^+ (T'_1 = 0 fs) and a slower component assigned to e^-_{sol} (T'_2 = 400 fs).

If we assume an absorption coefficient of 1.85×10^4 M^{-1} cm^{-1} for the solvated electron at 720 nm (Hall & Kenney-Wallace, 1978; Nikogosyan et al., 1983), the concentration of solvated electron produced after each femtosecond pulse is 17 ± 1 μM, assuming that the contribution of PTH^+ at this wavelength is less than 5%. From the extinction coefficients of e^-_{sol} and the cation radical PTH^+ at 520 nm (6×10^3 M^{-1} cm^{-1} and 6.5×10^3 M^{-1} cm^{-1}, respectively) (Alkaitis et al., 1975a), we deduce that 2 ps after the excitation the concentration of PTH^+ is comparable to the concentration of e^-_{sol} (17.8 μM). In neutral or acid micelles, no significant relaxation of the induced absorption at 520 and 720 nm (Figure 3) is observed in the first 350 ps. This indicates that the conversion of aqueous electron to H_2 via the bimolecular reaction (eq 4) and the reaction of e^-_{sol} with proton (eq 5) remain negligible in our experimental conditions.

$$e^-_{sol} + e^-_{sol} + 2H_2O \rightarrow H_2 + 2OH^- \quad (k = 5 \times 10^9\ M^{-1}\ s^{-1}) \tag{4}$$

$$e^-_{sol} + H_3O^+ \rightarrow H^\cdot + H_2O \quad (k = 2 \times 10^{10}\ M^{-1}\ s^{-1}) \tag{5}$$

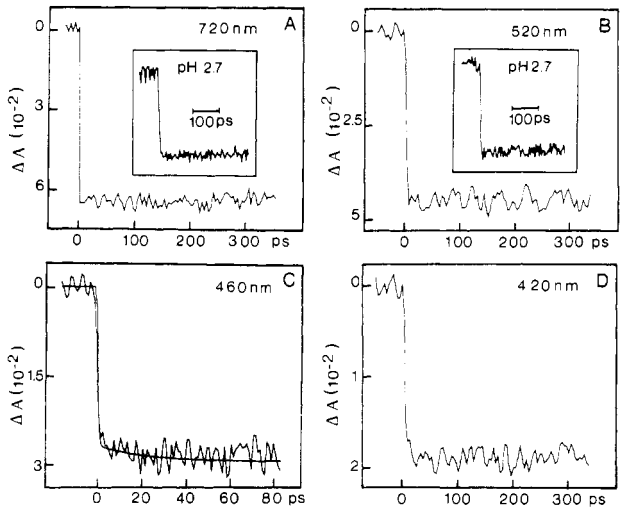

FIGURE 3: Set of time-resolved data showing the behavior of the induced absorption at 720 (A), 520 (B), 460 (C), and 420 nm (D) following the photoionization of PTH in anionic aqueous micelles ([PTH] = 2×10^{-4} M; [NaLS] = 0.07 M, pH 6.5). At 460 nm, the slow component can be well fitted to a monoexponential law (time constant = 18 ± 2 ps). The inserts in (A) and (B) show the induced absorption in acid anionic micelles (pH 2.7).

Time-resolved absorption at 460 nm shows a two-component rise. The first one (faster) corresponds to the appearance of e^-_{sol} and PTH^+. The other one (slower) is developed with a time constant of 18 ± 2 ps. This component has been assigned to a triplet state of PTH (Alkaitis et al., 1975a). Using an extinction coefficient for PTH_T* at 460 nm of 2.2×10^4 M^{-1} cm^{-1} in anionic micelles, we evaluate the concentration of PTH_T* to be 0.3 ± 0.1 μM, which is about 2% of the PTH^+ concentration.

Picosecond Kinetics of e^-_{sol} with Oxidized Pyridine Nucleotides. The reaction of e^-_{sol} with oxidized pyridine dinucleotide (NAD^+) or mononucleotide (NMN^+) was studied in anionic aqueous micelles. Figure 4 shows the transient absorption spectra following the photoionization of the redox system PTH/micelle/NAD^+ (0.08 M), pH 2.7. The spectrum obtained 2 ps after the excitation shows similarities with the one obtained without pyridine nucleotide (Figure 1), but with an additional hump at lower wavelengths. Two picoseconds after the femtosecond excitation an additional hump, centered on 450 nm, can be observed. While the overall transient absorption decays, this particular structure is still visible 9 ps after the excitation. The scheme of the reactions occurring in this synthetic and functional redox system, PTH/micelle/pyridine nucleotide, can in part be described by

$$[PTH]_M + [Pyr^+] \xrightarrow{h\nu} [PTH^+]_M + e^-_{presol} + [Pyr^+] \rightarrow [PTH^+]_M + e^-_{sol} + [Pyr^+] \quad (6)$$

$$e^-_{sol} + [Pyr^+] \underset{k_{-1}}{\overset{k_1}{\rightleftharpoons}} [Pyr^+ \cdots e^-_{sol}] \underset{k_{-2}}{\overset{k_2}{\rightleftharpoons}} Pyr^{\bullet} \quad (7)$$

The rate constant for the electron transfer with pyridine dinucleotide was determined by following the rate of disappearance of the e^-_{sol} absorption at 720 nm. Figure 5A shows a typical time-resolved electron transfer at pH 2.7. NAD^+ (0.101 M) reduces the lifetime of e^-_{sol}. Notice also a fast early relaxation in the first picoseconds following excitation, the nature of which will be discussed later. In the conditions where $[e^-_{sol}] \ll [NAD^+]$, the pseudo-first-order condition prevails, and the slower decay signal can indeed be fitted to a monoexponential with rate constant T_2 = 145 ± 5 ps. The kinetics obtained with NMN^+ in identical conditions are very similar (Figure 5B).

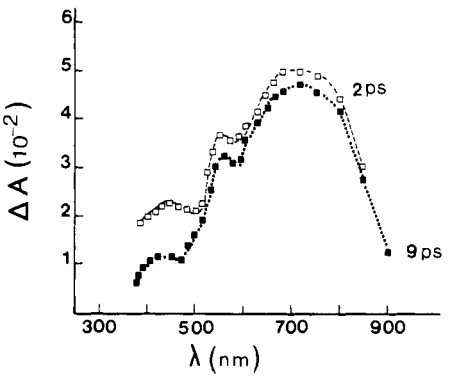

FIGURE 4: Transient absorption spectra 2 and 9 ps after the photoionization of PTH in deoxygenated anionic biomicelles ([PTH] = 2×10^{-4} M, [NaLS] = 0.07 M, NAD^+ = 0.1 M, pH 2.7).

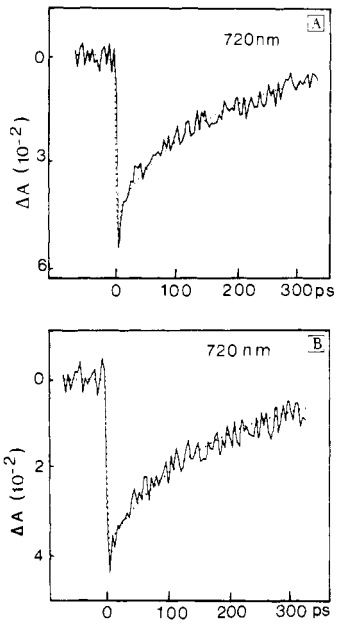

FIGURE 5: Time-resolved absorption following the photolysis of phenothiazine in anionic micelles. (A) Biomicelles containing NAD^+ ([PTH] = 2×10^{-4} M, [NaLS] = 0.07 M, [NAD^+] = 101 mM, pH 2.7). At 720 nm, the absorption decay is well fitted to a biexponential decay [$a \exp(-t/T_1) + b \exp(-t/T_2) + c$] with T_1 = 2.3 ± 0.2 ps and T_2 = 145 ± 5 ps. (B) Biomicelles containing NMN^+ ([PTH] = 2×10^{-4} M, [NaLS] = 0.07 M, [NMN^+] = 0.1 M, pH 2.7). The kinetics are fitted to a biexponential law with T_1 = 2.4 ± 0.2 ps and T_2 = 155 ± 5 ps.

Table I: Hydrated Electron Rate Constants in Biomicellar Systems: NaLS (0.07 M), PTH (2×10^{-4} M), and Pyridine Nucleotide (NAD^+ or NMN^+)

nucleotide	pH	concn (mM)	k (e^-_{sol} + pyridine) (M^{-1} s^{-1})
NAD^+	6.8	45	2.8×10^{10}
NMN^+	6.8	45	2.6×10^{10}
NAD^+	6.8	65	3.0×10^{10}
NMN^+	6.8	75	3.3×10^{10}
NAD^+	2.7	54	5.8×10^{10}
NMN^+	2.7	45	5.9×10^{10}
NAD^+	2.7	101	6.8×10^{10}
NMN^+	2.7	103	6.5×10^{10}

To study the reduction of pyridine mono- or dinucleotide in more detail, we have measured the apparent first-order rate constant ($k_{obsd} = 1/T$) of reaction 7 as a function of the concentration of pyridine nucleotide. Table I summarizes the bimolecular rate constant for reaction of e^-_{sol} with oxidized pyridine mono- or dinucleotide at pH 2.7 and 6.8. The second-order rate constant for the univalent reduction of pyridine nucleotide is faster in acid conditions than at neutral pH. The

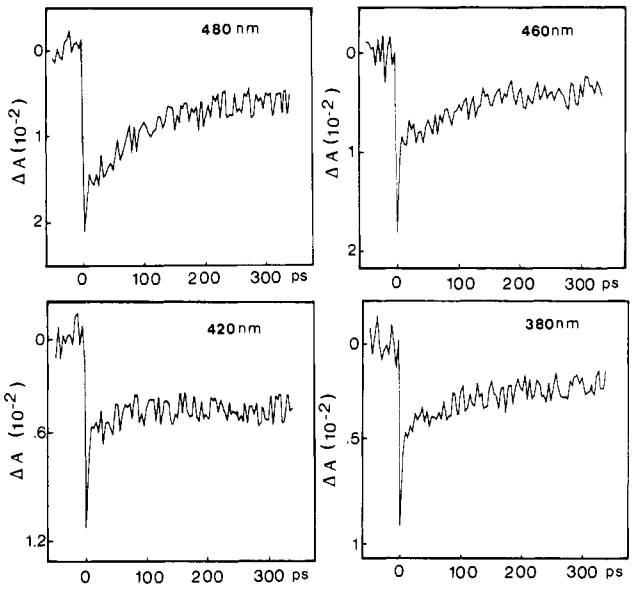

FIGURE 6: Induced absorption kinetics at 480, 460, 420, and 380 nm following the photoionization of PTH in anionic aqueous micelles ([PTH] = 2×10^{-4} M, [NaLS] = 0.07 M, [NAD^+] = 0.101 M, pH 2.7).

bimolecular rate constant changes also with the concentration of acceptor (Table I).

Spectral Identification of NAD• in Biomicelles. Dynamics scavenging experiments with NAD^+ were performed at different wavelengths to characterize the pyridinyl radical (NAD•). The analysis of the kinetics (Figure 6) has been performed with a model in which the optical density is computed by the eq 8, taking into account all the transient species

$$OD_{(\lambda)} = \sum_i C_i \epsilon_i l \qquad (8)$$

i (e^-_{sol}, PTH^+, PTH*, pyridinyl radical). We assume that the lifetime ($1/k_1$) of the encounter pair [e^-_{sol}:Pyr^+] is much shorter than $1/k_2$ (eq 7). Consequently, we can write

$$d[e^-_{sol}]/dt = -k_1[Pyr][e^-_{sol}] \qquad (9)$$

If [Pyr] $\gg$ [e^-_{sol}], $d[e^-_{sol}]/dt = -k_{obsd}[e^-_{sol}]$ and $[e^-_{sol}] = [e^-_{sol}]^0 \exp(-k_{obsd}t)$ with $k_{obsd} = 1/T = k_1$ [Pyr]. In this scheme, it is considered that e^-_{sol} interacts only with the pyridinyl compound and that the reaction of e^-_{sol} with other species (H^+, e^-_{sol}, PTH^+) remains, as previously shown, negligible at the picosecond time scale (eq 4 and 5).

The evolution of the pyridinyl radical (NAD•) follows the expression

$$[NAD^\bullet] = [e^-_{sol}]^0[1 - \exp(-k_{obsd}t)] \qquad (10)$$

The total optical density which includes the contribution of all the transient species, e^-_{sol}, PTH^+, NAD•, PTH*, is therefore

$$OD_{(t)} = [\epsilon_{e^-_{sol}}[e^-_{sol}]^0 \exp(-t/T_1) + \epsilon_{NAD\bullet}[e^-_{sol}]^0[1 - \exp(-t/T_1)] + \epsilon_{PTH_T\bullet}A[1 - \exp(-t/T')]]l \qquad (11)$$

A is the concentration of PTH_T*, T' is the time constant of appearance of PTH_T*, and l is the sample thickness. If the optical density is measured at two different times, the extinction coefficient of the pyridinyl radical ($\epsilon_{NAD\bullet}$) at a given wavelength can be calculated from the $OD_{(t_1)}/OD_{(t_2)}$ ratio:

$$\epsilon_{NAD\bullet} = \{\epsilon_{e^-_{sol}}[OD_2 \exp(-t_1/T) - OD_1 \exp(-t_2/T)] + \epsilon_{PTH^+}(OD_2 - OD_1) + \epsilon_{PTH\bullet}[(OD_2 - OD_1) + OD_1 \exp(-t_2/T') - OD_2 \exp(-t_1/T')]\}/\{(OD_1 - OD_2) - OD_1 \exp(-t_2/T) + OD_2 \exp(-t_1/T)\} \qquad (12)$$

Figure 7 shows the calculated values of the molecular extinction coefficient of the pyridinyl radical ($\epsilon_{NAD\bullet}$) for two pHs.

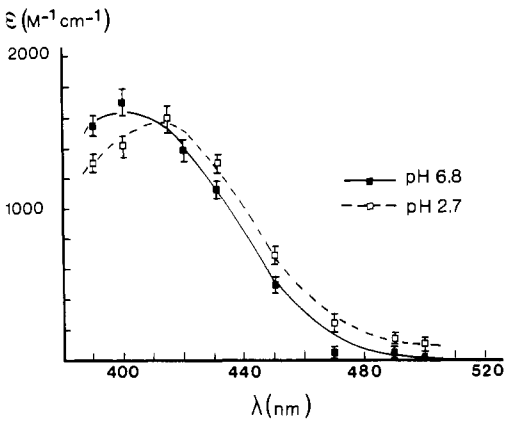

FIGURE 7: Absorption spectra of pyridinyl radical (NAD•) in biomicellar systems ([PTH] = 2×10^{-4} M, [NaSL] = 0.07 M, [NAD^+] = 0.08 M) for two pHs (2.7 and 6.8). At pH 6.8, the organized assemblies contained Tris–EDTA–borate buffer (0.02 M).

In neutral conditions (pH 6.7), the pyridinyl radical in micellar solution is characterized by an absorption band centered around 400 nm. The calculated molecular extinction coefficient equals 1850 ± 50 M^{-1} cm^{-1} at 400 nm. At the lower pH of 2.7, the calculated spectrum of the pyridinyl radical shows a slight shift of 15–20 nm toward the longer wavelengths, but the maximum extinction coefficient is similar to the value obtained in neutral conditions.

Theoretical Analysis of the Bimolecular Rate Constant (e^-_{sol} + Pyridine). In the redox system PTH/micelle/pyridine nucleotide, the rate constant (e^-_{sol} + pyridine dinucleotide) has been analyzed in a scheme of a diffusion-controlled reaction dependent on electrostatic and temporal factors. The rate constant at time t can be express as the formulation of Noyes (1961):

$$k_{(t)} = k_{00}\left(1 + \frac{k_{00}}{4\pi R_{ab}D_{ab}N \times 10^{-3}} \frac{R_{ab}}{(\pi D_{ab}t)^{1/2}}\right) \qquad (13)$$

It is considered that each molecule of reactant does not exert long-range forces and is distributed at random. R_{ab} is the reaction radius, i.e., the sum of the radius of the solvated electron and the pyridine nucleotide, D_{ab} is the diffusion coefficient for relative diffusion of e^-_{sol} and pyridine nucleotide, N equals Avogadro's number, and k_{00} is the rate constant of bimolecular reaction in dilute solutions. The value $k_{(t)}$ is computed for t equal to the half-lifetime of the reaction ($t_{1/2} = T \log 2$). At neutral pH, we have kept $k_{00}/(4\pi R_{ab}D_{ab}N \times 10^{-3})$ in eq 13 because electrostatic or steric factors intervene in the bimolecular rate constant. The diffusion-controlled encounter rate between uncharged spherical entities in dilute solution can be estimated by the Smoluchowski–Debye equation (Debye, 1942):

$$k_d = 4\pi D_{ab}R_{ab}N \times 10^{-3} \qquad (14)$$

For charged spherical particles, the extended theory takes into account the Coulombic interactions between charged species according to the Debye equation

$$k_d f_{elec} = k_{obsd} \qquad (15)$$

with f_{elec} being the electrostatic factor:

$$f_{elec} = \frac{Z_a Z_b e^2/kTR_{ab}\epsilon_r}{\exp(Z_a Z_b e^2/\epsilon_r kTR_{ab}) - 1} \qquad (16)$$

In this expression, ϵ_r is the static dielectric constant, k is the Boltzman constant, and T is the temperature (294 K). Z_a and Z_b are the units of electronic charge of solvated electron and pyridine nucleotide, respectively.

In the present study, let us consider the oxidized nucleotide (NAD^+) and e^-_{sol} as charged spherical species. The diffusion coefficient (D_x) of each reactant can be then deduced from the Nernst–Einstein relation: $kT/6\pi\eta R_x$, with η being the mean viscosity and R_x being the reaction radius. We have taken η equal to 0.89 as for bulk water, the radius of 2.5 Å for e^-_{sol}, and the diffusion coefficient 4.8×10^{-5} cm^{-1} s^{-1} (Delaire et al., 1980). In neutral biomicelles (pH 6.7), the net charge of the pyridine dinucleotide is −1. Its folded conformation allows this molecule to be considered as a spherical entity with a radius of 7 Å, yielding a diffusion coefficient of 0.345×10^{-5} cm^2 s^{-1}, value which is in agreement with experimental values defined by Bresnahan et al. (1981) and which corresponds to half of the ATP diffusion coefficient.

At neutral pH and at zero ionic strength, we find a rate constant k_d (e^-_{sol} + NAD^+) of 4.65×10^{10} M^{-1} s^{-1}. This value is greater than the experimental data obtained with pulse radiolysis of dilute solutions of NAD^+: $k = 2.5 \times 10^{10}$ M^{-1} s^{-1} (Land & Swallow, 1968). This experimental value is taken as equal to k_{00}. Inserting $\epsilon_r = 78$ for the aqueous phase of the micelle, eq 16, yields an electrostatic factor for NAD^+ of 0.612 at pH 6.8. From

$$k_{00} = k_d f_{elec} f_{ster} = F k_d \qquad (17)$$

and using $F = 0.531$ and $f_{elec} = 0.612$, one obtaines $f_{ster} = 0.87$.

When the oxidized pyridine dinucleotide is incorporated in acid micellar systems (pH 2.7), the purine base is protonated because the pK of adenine N_1H is 3.88 (Jardetzky & Wade-Jardeztsky, 1966). This perturbation increases the repulsion of the two positively charged rings and therefore favors the existence of an unfolded configuration (Hamill et al., 1974). Considering that the longer distance between the two rings (pyridinium ion and protonated adenine) is about 10 Å, the radius of the molecular sphere has been estimated to 9.33 Å, and the calculated diffusion constant equals 0.268×10^{-5} cm^2 s^{-1}. At pH 2.7, the total charge of the nucleotide is zero owing to the fact (1) that N_1 of adenine is protonated and (ii) that the phosphate groups remain dissociated (pK = 1.7). The estimate of k_{00} in acid conditions is obtained by the Smoluchowski–Debye equation (eq 14). Under the assumption that the steric factor (0.87) is not significantly influenced by the pH, we obtained $k_d = 4.41 \times 10^{10}$ M^{-1} s^{-1} and $k_{00} = 3.84 \times 10^{10}$ M^{-1} s^{-1}. This value is reported in eq 13 to calculate the concentration-dependent rate constant in acid biomicellar systems.

The ionic strength (μ) linked to the ionic atmosphere around e^-_{sol} or NAD^+ is able to reduce the Coulombic interactions. The formulation of Brønsted, Bjerrun, and Debye-Hückels accounts for the variation of the rate constant $k_{(t)}$ with the ionic strength:

$$\log (k/k_0) = \frac{1.02 Z_a Z_b \mu^{1/2}}{1 + Ba\mu^{1/2}} \qquad (18)$$

in which k is the rate constant at ionic strength μ and k_0 is the rate constant at zero ionic strength, a is the distance of closest approach of charged species, and $B = 0.329$ in water at 294 K (Jonah et al., 1975). This ionic strength effect can be influenced by the time necessary for the ionic atmosphere to form around e^-_{sol}. This time is determined from Coyle et al. (1964):

$$T_r = \frac{(3.55 \times 10^{-9}) \sum_j Z_j}{\mu \sum_j \Lambda_j} \qquad (19)$$

in which T_r is expressed in picoseconds and Λ_j is the equivalent conductance of each type of ion in the solution. By use of the limiting equivalent conductance of e^-_{sol} (170 cm^2 Ω^{-1} $equiv^{-1}$) (Matheson, 1965) and of Na^+ (45 cm^2 Ω^{-1} $equiv^{-1}$) (Robinson & Stokes, 1959), the relaxation time of the ionic atmosphere of e^-_{sol} is found to be 290 ps. This time is longer than the experimental half-lifetime of the reaction e^-_{sol} + NAD^+ ($t_{1/2}$ = log $2T$ = 215 ps for NAD^+, 0.101 M, pH 6.7).

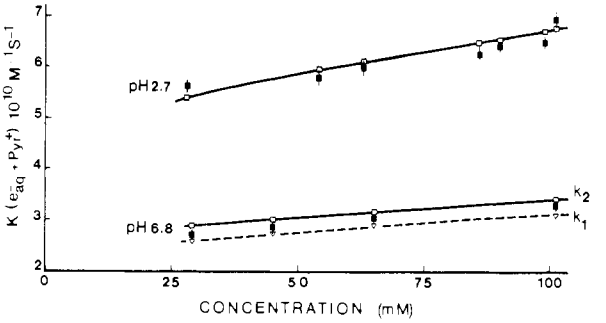

FIGURE 8: Variation of k (e^-_{sol} + nucleotide) with concentration (mM) of nicotinamide adenine dinucleotide for two pHs (2.7 and 6.8). The solid curves are calculated from eq 13–19, which take into account the time dependence and steric and electrostatic factors. (■) Experimental data; (▽, □) theoretical rate constant (k_1, k_2).

The calculated values of $k_{(t)}$ for the different conditions of NAD^+ concentration and pH are reported in Figure 8. This figures shows that at pH 2.7 the estimates of $k_{(t)}$ are in good agreement with the experimental rate constants measured at the picosecond time scale. At neutral pH, the calculated values of $k_{(t)}$ are lower than those in acids conditions. We have plotted the value of k_1 and k_2 representing the cases where the ionic atmosphere around e^-_{sol} is at equilibrium (k_2) or not (k_1). From these calculated data, we conclude that at neutral pH the ionic strength effect on the univalent reduction of NAD^+ remains weak.

Ultrafast Formation of Pyridinyl Radical in Biomicelles. The transient spectra have been reconstructed for delays of 2 and 9 ps after excitation of the PTH/micelle/NAD^+ system, pH 2.7 (Figure 4). They show a specific hump centered around 420 nm and a broad band which rapidly decays. A deconvolution analysis of the induced absorption in the 650–900-nm spectral range indicates two buildup times (Figure 9). In biomicelles with NAD^+ or NMN^+, the first rise time appears in less than 50 fs while the second component has a time constant of 400 ± 20 fs (Figure 9C,D). This last kinetics is identical with the rate of electron solvation in micelles without oxidized coenzyme or AMP (Figure 9A,B).

As it has been shown previously (Figures 5 and 9), a significant decay of the transient absorption occurs within the first picoseconds following excitation. At pH 2.7, this fast decay at 720-nm absorption can be fitted to a monoexponential law with a time constant of 2.3 ± 0.2 ps (Figure 10A). Identical time constants are obtained at pH 6.8 and for biomicelles containing NMN^+ (Figure 10B,C). By contrast, no relaxation is observed with adenosine monophosphate (Figure 10D). The different contributions of the induced absorption in the range 400–500 nm have been carefully analyzed in Figure 11. This figure shows the differential transient spectrum obtained by numerically removing the contribution of e^-_{sol} and PTH^+ established at 2 ps. Two picoseconds after the femtosecond laser pulse, the early hump around 440 nm is superimposed to a large background which rapidly decays. We tentatively assigned the previous broad structureless band, observed also in aqueous solution of NAD^+, to an excited state of nicotinamide, $(Pyr^+)^*$. The narrower band peaking around 420 nm is similar to the previously

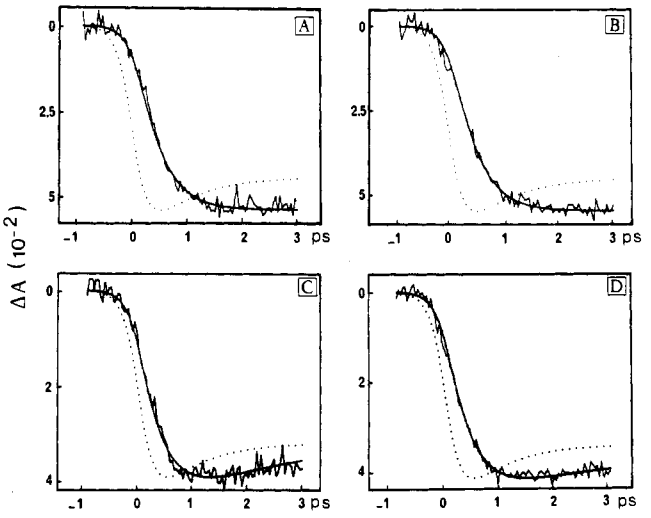

FIGURE 9: Rise of the induced absorption at 720 nm following the photoionization of PTH (2×10^{-4} M). (A) Micellar systems ([NaSL] = 0.07 M). (B) Biomicelles + AMP (0.1 M). (C) Biomicelles + NMN^+ (0.1 M). (D) Biomicelles + NAD^+ (0.1 M). (A and C) The deconvolution analysis yields a rise time of 410 fs. The signal buildup in (C) and (D) can be described with two components: an instantaneous response (i.e., 100 fs) relaxing in 2.5 ps and a rise time of 400 ± 20 fs. The instantaneous responses (···) are defined by recording an induced absorption after excitation of pure liquid *n*-heptane.

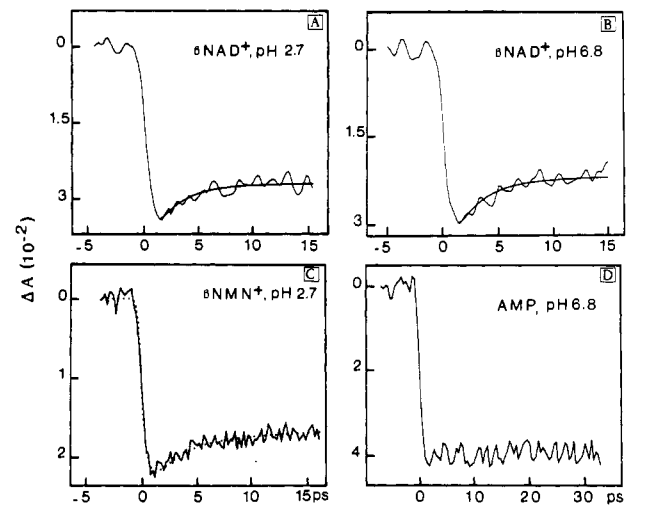

FIGURE 10: Transient absorbance at 720 nm showing the decay of the signal after the photoionization of PTH in anionic biomicellar systems ([PTH] = 2×10^{-4} M, [NaLS] = 0.07 M). (A) $[NAD^+]$ = 0.01 M, pH 2.7; (B) $[NAD^+]$ = 0.1 M, pH 6.8; (C) $[NMN^+]$ = 0.1 M, pH 2.7; (D) [AMP] = 0.1 M, pH 6.8. The kinetics of the absorption decays at 720 nm (A–C) are fitted to a monoexponential law with $T = 2.3 \pm 0.2$ ps.

calculated spectrum of the pyridinyl radical $NAD^•$ following the reaction of e^-_{sol} with NAD^+ (Figure 8). This suggested that this hump could be attributed to a fast formation of a pyridinyl radical ($NAD^•$). Knowing the calculated extinction coefficient for $NAD^•$ at 420 nm in a micellar system (1.85×10^3 M^{-1} cm^{-1}), it is possible to evaluate the concentration of the free radical $NAD^•$ produced through this ultrafast electron transfer. We obtained approximately, at 2 ps, $[NAD^•] = 2.1 \pm 0.2\ 10^{-6}$ M, i.e., less than 10% of the total pyridinyl formation. It can be noticed that 2 ps after the photoionization of PTH the quantity of e^-_{sol} which has been able to react with the pyridinyl nucleotide is about 0.15 μM.

Discussion

Charge Separation in Anionic Micelles. The present experiments have directly determined the dynamics of the early

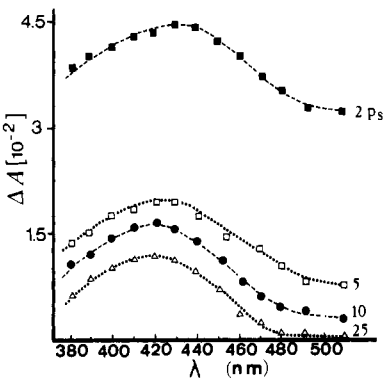

FIGURE 11: Picosecond differential spectra obtained following the photolysis of PTH in biomicellar systems: [PTH] = 2×10^{-4} M; [NaLS] = 0.07 M; $[NAD^+]$ = 0.07 M; pH 2.7.

events leading to the formation of the solvated electron (e^-_{sol}) in anionic aqueous micelles. The interaction of intense UV laser pulses with PTH which has a low ionization potential (I_g = 6.5 eV) leads to an ultrafast charge separation ($PTH^+ \cdots e^-$) inside the micelle and the subsequent electron transfer across the hydrocarbon phase. The primary ionization step ($PTH^+ \cdots e^-$) occurs with a time constant which is limited by the instrumental response, i.e., less than 10^{-13} s. Two distinct hypotheses may be considered to account for the ionization process of PTH when high-intensity excitation is used. The first one, considered by Alkaitis et al. (1975) with nanosecond photolysis experiments, would correspond to a monophotonic ionization of PTH. The absorption of 4 eV would lead to a vibrationally excited level in the first excited singlet state PTH_{S1} (2.9 eV above the ground state). Since at this energy the density of the unoccupied level of the system aq/e^-_{aq} is high, it has been suggested that an electron can rapidly tunnel from this excited state of PTH to the perimicellar aqueous phase (Alkaitis et al., 1975). The second hypothesis would involve either a two-step process in which a second photon will be absorbed by the singlet state S_1 of PTH or a direct two-photon excitation.

In the specific case of anionic aqueous micelles, the femtosecond photolysis channel of PTH is relevant of a common highly excited state which either ionizes or relaxes toward another excited state and especially a long-lived triplet state. In accordance with the nanosecond experiments of Alkaitis et al. (1975), the proportion of triplet formation vs e^-_{sol} following femtosecond photolysis is low in aqueous micelles. This fact can be explained by the repulsive effect of the interfacial electric potential (ψ_i) which prevents the recombination of geminate ion pairs (eq 1). Consequently, triplet formation does not derive from the recombination of the geminate ion pair $[PTH^+ \cdots e^-_{qf}]$. The weak formation of PTH_T in the photoionization channel of PTH can also be in agreement with a biphotonic process in which the intersystem crossing to the triplet state will be less important than a radiative deactivation of the Franck–Condon highly excited singlet state.

It is clear that the solvation of the photoelectron in the perimicellar phase does not proceed through a single step because a presolvated state of electron absorbing in the infrared is identified. The rise time T_1 of the infrared tail (250 fs) includes the ejection of the electron from the hydrophobic inner core of the micelle, thermalization, and the trapping of the electron in the aqueous phase. During these different steps, the electron must pass through the hydrocarbon chain of surfactant molecules and overcome the potential barrier of the interfacial layer (Stern layer). From the comparison with rise time T_1 (T_1 = 110 fs) obtained after two-photon ionization

of liquid water (Gauduel et al., 1986; Migus et al., 1987), it is apparent that the rate of formation of the precursor of e^-_{sol} is lengthened in the micellar aqueous phase. This difference can be explained by the existence of a gradient ion concentration in the vicinity of micelles (Stern layer). The electric potential profile (ψ_i) inside the Gouy–Chapman layer constrains the electron localization to occur at 35–40 Å outside the micellar surface (Grätzel & Thomas, 1974). This means that the presolvation of electron occurs in a region which has no specific structure imposed by the interfacial layer. Once the electron gets trapped, the final stabilization of this presolvated state occurs following a single step with a rate constant of 270 fs. This similitude between the time T_2 and the electron solvation time in pure water (240 fs) suggests (i) that the energy loss mechanism of presolvated electron is comparable in liquid water and aqueous micelles and (ii) that the initial presolvated and final e^-_{sol} correspond to two separate electronic states. The spectrum of e^-_{sol} in micellar phase being similar to that in pure aqueous solution, it can be concluded that the electron solvation occurs in the outer Gouy–Chapman layer, i.e., in a region where local dielectric constant is similar to that of bulk water and higher than that at the micellar interface (Thomas, 1980).

The fact that 2 ps after the laser excitation the concentration of the cationic radical (PTH^+) is similar to that of the solvated electron indicates that all the photoelectrons which are ejected through the charged interface become solvated in the polar aqueous phase. It is interesting to notice that in the first few hundred femtoseconds following charge separation no discernible geminate recombination occurs between the PTH^+ radical and the nonfully hydrated electron. This result does not preclude that ultrafast intramicellar geminate recombination of the ion pair ($PTH^+ \cdots e^-$) actually occurs during the 100-fs pulse duration. In this hypothesis, an intramicellar geminate recombination will be a determinant factor of the initial photoionization yield (ϕ_{e^-}). This primary photoionization yield is a complex parameter which includes both a primary ionization cross-section term (φ_{ip}) and an electron escape probability W: $\phi_{e^-} = \varphi_{ip} W$. A priori, it is difficult to decide which of these two terms, or both, is affected by a variation of the surface electric potential (ψ_i) (Bernas et al., 1986; Grand et al., 1983). Femtosecond studies are in progress to understand the influence of ψ_i on the early photoionization and electron-transfer process in micelles.

Kinetics of Free-Radical Reactions with Pyridine Nucleotides. The incorporation of nucleotides (NAD^+, NMN^+) in the aqueous phases of anionic micelles leads to a redox system which allows a cation radical (PTH^+) effect on the kinetics of monoelectronic transfer to be avoided. The hydrophilic properties of these coenzymes at neutral and acid pH would favor their solubilization in the polar phase of the micelles. The static UV spectral data of the nucleotides in biomicelles are similar to control values obtained in homogeneous aqueous solutions and no spectral shift of the optical absorption maximum of the micellized chromophore is observed in biomicelles. These spectral observations tend to indicate that in the anionic NaLS micelles the probability that an electron donor (PTH) and an acceptor (pyridine nucleotide) are in close proximity remains low.

In our conditions, the femtosecond photoionization of PTH in the redox system PTH/micelle/pyridine nucleotides initiates a one-electron-transfer reaction (Figure 11) leading to the formation of a pyridinyl radical ($Pyr^•$). At neutral pH, the net charge of the dinucleotide being −1, it can be assumed that this oxidized cofactor is localized far from the electric potential ($\psi_i = -70$ mV) of the micellar surface. Therefore, neither the electric field of the Stern layer nor the Gouy–Chapman layer should perturb the univalent reduction and the electronic environment of the radical ($Pyr^•$). This conclusion is confirmed by the fact that the calculated spectrum of the semiquinone exhibits an absorption band which is similar to the microsecond spectrum in dilute solutions. The extinction coefficient at 400 nm ($\epsilon_{NAD•} = 1.85 \times 10^3$ M^{-1} cm^{-1}) agrees well with these previous experimental spectral data (Land & Swallow, 1968, 1971). In agreement with Hamill et al. (1974) and Sarma and Mynott (1973), our experiments demonstrate the absence of a significant aggregate between nucleotides in the range of concentration 0.025–0.1 M.

In acid biomicelles (pH 2.7), the transient spectrum of the pyridinyl radical shifts about 15–20 nm toward the red (Figure 8). This effect has not been observed by other authors in acid aqueous solution. Therefore, these authors concluded that the pK of $NAD^•$ was less than 0.3 (Kosower et al., 1978). The slight discrepancy between these results and ours may be due to differences in the molecular environment (high concentration of nucleotides). Since there is no significant change either in the molar absorbance or in the profile of the calculated spectrum, it may be assumed that in acid biomicelles the $NAD^•$ radical retains its integrity. The picosecond kinetic data show that the reaction of e^-_{sol} with oxidized coenzymes (NAD^+, NMN^+) proceeds through a one-electron-step reaction, and experimental kinetics exhibit a pseudo-first-order rate constant. The analysis of the pH effect permits the conclusion that protonation of the adenine ring influences the diffusion-controlled reaction through electrostatic effects.

Owing to the fact that most of free-radical reactions have a low activation energy ($\Delta E = 3$ kcal mol^{-1}), the rate constant for the reaction of e^-_{sol} with pyridine nucleotide ($k > 10^{10}$ M^{-1} s^{-1}) is indicative of a diffusion-controlled process where practically every encounter yields a product. The absolute rate constant of the scavenging reaction depends very little upon the nature of the nucleotide (mono- or dinucleotide). This result suggests that the nicotinamide ring is the main point of attack of the electron and the site of reduction. However, the two nicotinamide and adenine rings being largely exposed to the solvent, it cannot be rejected that adenine is another initial point of attack in NAD^+ and that an electron rapidly transfers to the nicotinamide ring through an intramolecular transfer (Land & Swallow, 1968). This mechanism is not unlikely at pH 6.8 because (i) adenine presents a high affinity for e^-_{sol} ($k = 1.2 \times 10^{10}$ M^{-1} s^{-1}) and (ii) the distance between the two rings (nicotinamide and adenine) is small, about 3.9 Å (Sarma et al., 1968).

The calculated bimolecular rate constant for different nucleotides concentrations shows a concentration dependence in the range 0.025–0.1 M (Table I). For the lower concentrations in neutral conditions, the bimolecular rate constant k (e^-_{sol} + NAD^+) is in agreement with the data obtained by pulse radiolysis of dilute solutions (Land & Swallow, 1968). So, there is no significant influence of dimerization of $NAD^•$ on the free-radical reaction, and the repartition of NAD^+ is homogeneous in the aqueous phase of the biomicelles. This is also valid in acid conditions because low pH reduces the lifetime of the dimer (Schmakel et al., 1975). At higher concentrations, several factors may favor a difference between the observed and the true bimolecular rate constant.

The analysis of the kinetics with Noyes' equations demonstrates (i) a concentration dependence of the rate of the univalent reduction of NAD^+ and (ii) that the monoelectronic transfer occurs when e^-_{sol} and the nucleotide are in physical

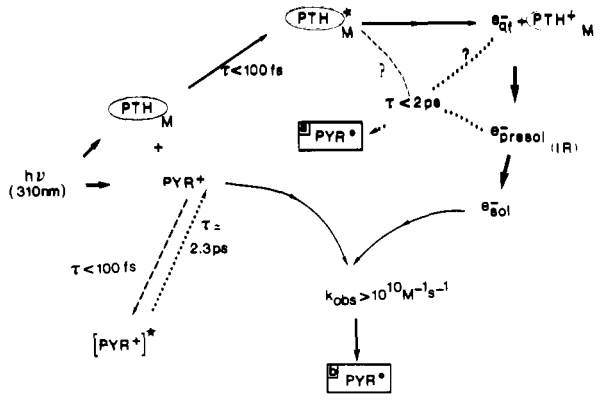

FIGURE 12: Schematic representation of reactions occurring in biomicelles (NaLS/PTH/NAD$^+$) following femtosecond UV photoionization of PTH. This figure shows the two channels (a and b) leading to the formation of the pyridinyl radical, NAD•.

contact, i.e., when the radius of reaction equals the sum of the radius of e^-_{sol} and that of pyridine nucleotide. This does not exclude that electron transfer on the vacant site in nucleotide occurs on a few angströms through a tunneling mechanism. In the micellar region where the electron transfer occurs, it can be concluded that the mobility of e^-_{sol} ($\mu = 2 \times 10^{-3}$ cm^2 V^{-1} s^{-1}), the dielectric constant ($\epsilon_r = 78$), and the viscosity ($\eta = 0.9$ cP) are similar to the values of bulk solution. We can also conclude that 2.5 Å is a good approximation of the reaction radius of e^-_{sol}.

Notice also that in the PTH/micelle/NAD$^+$ system an early relaxation (2.3 ± 0.2 ps) is apparent in the red spectral region. Among other hypotheses, this relaxation may be attributed to the spectral contribution of an encounter pair (e^-_{sol}:Pyr$^+$). Previously, Czapski and Peled (1973) have suggested that the reduction of the initial yield of e^-_{sol} in concentrated solutions could be explained by the direct formation of an encounter pair linked to the solvation of electron in the reaction radius of scavenger. Lam and Hunt (1975) predicted that the lifetime of the encounter pair must be less than 10^{-11} s. Our experimental relaxation time (2.3 ps) agrees with this estimate. However, several arguments stand against a clear assignment of the transient broad band in the visible to a fast formation of an encounter pair (e^-_{sol}:Pyr$^+ \rightarrow$ Pyr•). The most convincing is that the probability P' of e^-_{sol} to be inside the encounter volume, $P' = 1 - \exp(4\pi r_{eff}^3[S]/10^3)$, is close to zero when the concentration of the pyridine nucleotide is 0.1 M (Lam & Hung, 1975).

On the other hand, we cannot completely exclude the spectral contribution of a solvated ion pair (e^-:Pyr$^+$) since biphotonic ionization of NADH has been observed at the nanosecond time scale (Czochralska & Lindquist, 1983).

The absence of a fast relaxation with adenosine monophosphate (AMP) tends to indicate that the transient 2.3-ps absorption can be assigned to a light-induced electronic excitation of the nicotinamide ring which slightly absorbs at 310 nm and whose the lifetime will then be in agreement with the upper limit of 10 ps as estimated by Lamola (1967). It can be noticed that if the deactivation of this excited state occurs through an intramolecular geometrical relaxation, there is no evidence for a significant role of adenine because the relaxation time at 720 nm is similar for NAD$^+$ and NMN$^+$. A reorientation of the solvent cage or charge-transfer complex can be suggested as a deactivation process of this excited state. The contribution of different populations of excited state attributed to distinct conformers or solvated nicotinamide moieties cannot be excluded because the transients show up on a broad spectral range.

One of the main results of the present study is the observation of an ultrafast buildup of spectral band around 420 nm following the femtosecond photochemical charge transfer. We give an upper limit of 2 ps for this ultrafast free-radical reaction with NAD$^+$. The analysis of C_{37} values with picosecond radiolysis of concentrated solutions has previously suggested that precursors of e^-_{sol} are able to react with solute molecules (Wolff et al., 1971; Aldrich et al., 1975; Jonah et al., 1977). Data of Aldrich et al. (1975) strongly suggest that nucleotides which have a small value of C_{37} can react with a precursor of e^-_{sol}. Our experimental results are also in agreement with a mechanism in which a precursor of e^-_{sol} takes part in the free-radical reactions with pyridine nucleotide at high concentration, with an upper limit of the rate of the free-radical reaction (pre-e^-_{sol} + Pyr$^+ \rightarrow$ Pyr•) of 5×10^{11} s^{-1}. The fact that the spectral data of the primary semiquinone (Pyr•) are very similar to those observed at the picosecond time scale with e^-_{sol} would then suggest that a precursor of e^-_{sol} attacks the same site as e^-_{sol} does on the pyridine nucleotide. From the present time-resolved spectral data, we cannot also exclude that a relaxation of the ion pair (pre-e^-_{sol}···NAD$^+$) occurs through an ultrafast electronic redistribution or reorganization of the solvation shell of the radical. Such an energy loss mechanism of the excited pyridinyl radical (Pyr•) would contribute to complicate the spectral evolution of the early band assigned to this radical.

Another hypothesis (Figure 12) will be that, in biomicelles where the [nucleotide]/[micelle] ratio is about 100, a small fraction of nucleotide molecules is solubilized in the periphery of the micellar surface or is closely associated with the negatively charged Stern layer. An ultrafast free-radical reaction coupled to a one-electron transfer can be considered between an excited state of phenothiazine (i.e., an extended Rydberg state) and the pyridine nucleotide. As it has been previously suggested by Grätzel and Thomas (1974), such a reactional process would compete with photoejection and presolvation of electron.

Further investigations in the infrared spectrum are in progress to establish the contribution of the different precursors of e^-_{sol} (thermalized or e^-_{presol}) in the ultrafast univalent reduction of nucleotides and to provide accurate kinetics of free-radical reactions which compete with electron hydration.

In conclusion, we have shown that femtosecond photochemical generation of electrons in anionic aqueous micelles yields direct spectral evidence of the existence of a presolvated state of electron at 294 K. The femtosecond initiation of the monoelectronic trasnfer leads to subsequent free-radical reactions in which e^-_{sol} is involved. The attachment of a solvated electron to an oxidized coenzyme (NAD$^+$) corresponds to a bimolecular diffusion-limited process ($k > 10^{10}$ M^{-1} s^{-1}). This experimental work demonstrates for the first time that an ultrafast free-radical reaction occurs faster than 5×10^{11} s^{-1}.

ACKNOWLEDGMENTS

We thank Drs. A. Bernas and S. Hautecloque for stimulating discussions and critical reading of the manuscript.

Registry No. NAD, 53-84-9; NMN, 1094-61-7; NAD•, 50958-71-9; phenothiazine, 92-84-2.

REFERENCES

Aldrich, J. E., Bronskill, M. J., Wolff, R. K., & Hunt, J. W. (1971) *J. Chem. Phys. 55*, 530–539.

Aldrich, J. E., Lam, K. Y., Shragge, P. C., & Hunt, J. W. (1975) *Radiat. Res. 63*, 42–52.

Alkaitis, S. A., Beck, G., & Grätzel, M. (1975a) *J. Am. Chem. Soc. 97*, 5723–5728.

Alkaitis, S. A., Grätzel, M., & Henglein, A. (1975b) *Ber. Bunsen-Ges. Phys. Chem. 79*, 541–546.
Anbar, M. (1969) *Adv. Phys. Org. Chem. 7*, 115–148.
Anbar, M., & Neta, P. (1967) *Int. J. Appl. Radiat. Isot. 18*, 493.
Bernas, A., Grand, D., Hautecloque, S., & Giannotti, C. (1986) *J. Phys. Chem. 90*, 6189–6194.
Beuhlmann, V., & Hayon, E. (1974) *J. Am. Chem. Soc. 96*, 6169–6175.
Bielski, B. H. J., & Chan, P. C. (1980) *J. Am. Chem. Soc. 102*, 1713–1717.
Bresnahan, E. M., & Elving, P. J. (1981) *J. Am. Chem. Soc. 103*, 2379–2386.
Bronskill, M. J., Wolff, R. K., & Hunt, J. W. (1970) *J. Chem. Phys. 53*, 4201–4210.
Catterall, W. A., Hollis, D. P., & Walter, C. F. (1969) *Biochemistry 8*, 4032–4036.
Chase, W. J., & Hunt, J. W. (1975) *J. Phys. Chem. 79*, 2835–2844.
Coyle, P. J., Dainton, F. S., & Logan, S. R. (1964) *Proc. Chem. Soc., London 219*.
Czapski, G., & Peled, E. J. (1973) *J. Phys. Chem. 73*, 893–897.
Czochralska, B., & Lindqvist, L. (1983) *Chem. Phys. Lett. 101*, 297–299.
Dainton, F. S. (1975) *Chem. Soc. Rev. 4*, 323–362.
Debye, P. (1942) *Trans. Electrochem. Soc. 82*, 265.
Delaire, J. A., Delcourt, M. O., & Belloni, J. (1980) *J. Phys. Chem. 84*, 1186–1189.
Duplatre, G., & Jonah, C. D. (1985) *Radiat. Phys. Chem. 24*, 557–565.
Falkenhagen, H. (1971) *Theorie der Elektrolyte*, p 120, Hirzel, Stuttgart, West Germany.
Fork, R. L., Shank, C. V., & Yen, R. T. (1982) *Appl. Phys. Lett. 41*, 223.
Gauduel, Y., Migus, A., Martin, J. L., & Antonetti, A. (1985) *Ber. Bunsen-Ges. Phys. Chem. 89*, 218–222.
Gauduel, Y., Martin, J. L., Migus, A., Yamada, N., & Antonetti, A. (1986) *Ultrafast Phenomena* (Fleming, G. R., & Siegman, A. E., Eds.) pp 308–311, Springer-Verlag, New York.
Grand, D., Hautecloque, G., Bernas, A., & Petit, A. (1983) *J. Phys. Chem. 87*, 5236–5240.
Grätzel, M., & Thomas, J. K. (1974) *J. Phys. Chem. 78*, 2248–2254.
Hall, G. E., & Kenney-Wallace, G. A. (1978) *Chem. Phys. 32*, 313.
Hamill, W. D., Pugmire, R. J., & Grant, D. M. (1974) *J. Am. Chem. Soc. 96*, 2885–2887.
Hart, E. J., & Anbar, M. (1970) *The Hydrated Electron*, Wiley-Interscience, New York.
Jardetzky, O., & Wade-Jardetzky, N. G. (1966) *J. Biol. Chem. 241*, 85.
Jonah, C. D., Miller, J. R., & Matheson, M. S. (1977) *J. Phys. Chem. 81*, 1618–1622.
Klapper, M. H., & Faraggi, M. (1983) *Biochemistry 22*, 4067–4071.
Kosower, E. M., Teuerstein, A., Burrows, H. D., & Swallow, A. J. (1978) *J. Am. Chem. Soc. 100*, 5185–5190.
Lam, K. Y., & Hunt, J. W. (1975) *Int. J. Radiat. Phys. Chem. 7*, 317–338.
Lamola, A. A. (1973) *Pure Appl. Chem. 34*, 281–303.
Land, E. J., & Swallow, A. (1968) *Biochim. Biophys. Acta 162*, 327–337.
Lewis, M. A., & Jonah, C. D. (1986) *J. Phys. Chem. 90*, 5367–5372.
Lichtin, N. N., Shafferman, A., & Stein, G. (1973) *Biochim. Biophys. Acta 314*, 117.
Logan, S. R. (1967) *Trans. Faraday Soc. 63*, 3004.
Matheson, I. B. C., & Rodgers, M. A. J. (1982) *J. Phys. Chem. 86*, 884–887.
Mialocq, J. C., Sutton, J., & Goujon, P. (1980) *J. Chem. Phys. 72*, 6238–6354.
Migus, A., Antonetti, A., Etchepare, J., Hulin, D., & Orszag, A. (1985) *J. Opt. Soc. Am. B: Opt. Phys. 2*, 584–594.
Migus, A., Gauduel, Y., Martin, J. L., & Antonetti, A. (1987) *Phys. Rev. Lett. 58*, 1559–1562.
Moroi, Y., Braun, A. M., & Grätzel, M. (1979) *J. Am. Chem. Soc. 101*, 567–572.
Nikogosyan, D. N., Oraevsky, A. A., & Rupasov, V. I. (1983) *Chem. Phys. 77*, 131–143.
Noyes, R. M. (1961) *Prog. React. Kinet. 1*, 129–160.
Pileni, M. P., Hickel, B., Ferradini, C., & Pucheault, J. (1982) *Chem. Phys. Lett. 92*, 308–312.
Razem, D., & Hamill, W. H. (1977) *J. Phys. Chem. 81*, 1625–1631.
Robinson, R. A., & Stokes, R. H. (1959) *Electrolyte Solutions*, p 44, Butterworths, London.
Sarma, R. H., & Mynott, R. J. (1973) *J. Am. Chem. Soc. 95*, 1641–1649.
Sarma, R. H., Ross, V., & Kaplan, N. O. (1968) *Biochemistry 7*, 3052–3062.
Schmakel, C. O., Santhanam, K. S. V., & Elving, P. J. (1975) *J. Am. Chem. Soc. 97*, 5083–5092.
Schwartz, H. A. (1971) *J. Chem. Phys. 55*, 3647–3650.
Thomas, J. K. (1980) *Chem. Rev. 80*, 284–298.
Thomas, J. K., Grieser, F., & Wong, M. (1978) *Ber. Bunsen-Ges. Phys. Chem. 82*, 937–949.
Visser, A. J. W. G., & Fendler, J. H. (1982) *J. Phys. Chem. 86*, 947–950.
Wallace, S. C., Grätzel, M., & Thomas, J. K. (1973) *Chem. Phys. Lett. 23*, 359–362.
Webb, J. W., Janik, B., & Elving, P. J. (1973) *J. Am. Chem. Soc. 95*, 991.
Wolff, R. K., Bronskill, M. J., & Hunt, J. W. (1970) *J. Chem. Phys. 53*, 4211–4215.
Wong, M., Grätzel, M., & Thomas, J. K. (1975) *Chem. Phys. Lett. 30*, 329–333.
Zana, R., Yiv, S., Strazielle, C., & Lianos, P. (1981) *J. Colloid Interface Sci. 80*, 208–213.